

OPTIMAL LEVERAGING OF SMOOTHNESS AND STRONG CONVEXITY FOR PEACEMAN–RACHFORD SPLITTING

LUIS BRICEÑO-ARIAS[‡] AND FERNANDO ROLDÁN[†]

ABSTRACT. In this paper, we introduce a simple methodology to leverage strong convexity and smoothness in order to obtain an optimal linear convergence rate for the Peaceman–Rachford splitting (PRS) scheme applied to optimization problems involving two smooth strongly convex functions. The approach consists of adding and subtracting suitable quadratic terms from one function to the other so as to redistribute strong convexity in the primal formulation and smoothness in the dual formulation. This yields an equivalent modified optimization problem in which each term has adjustable levels of strong convexity and smoothness. In this setting, the Peaceman–Rachford splitting method converges linearly to the solution of the modified problem with a convergence rate that can be optimized with respect to the introduced parameters. Upon returning to the original formulation, this procedure gives rise to a modified variant of PRS. The optimal linear rate established in this work is strictly better than the best rates previously available in the general setting. The practical performance of the method is illustrated through an academic example and applications in image processing.

Keywords. *Convex analysis, Convergence rate, Duality, Fenchel conjugate, Peaceman–Rachford splitting, Proximal splitting algorithms*

2020 *Mathematics Subject Classification.* 47H05, 65K05 65K15, 90C25.

1. INTRODUCTION

This paper is devoted to the efficient resolution of the following convex optimization problem defined in a real Hilbert space \mathcal{H} . We denote by $\Gamma_0(\mathcal{H})$ the class of lower semicontinuous convex proper functions from \mathcal{H} to $]-\infty, +\infty]$, given $h \in \Gamma_0(\mathcal{H})$, ∂h denotes its subdifferential, and h is γ -strongly convex for some $\gamma \geq 0$ if $h - \gamma \|\cdot\|^2/2$ is convex.

Problem 1.1. *Let $\rho \geq 0$ and $\mu \geq 0$, let $f \in \Gamma_0(\mathcal{H})$ and $g \in \Gamma_0(\mathcal{H})$ be ρ and μ -strongly convex functions, respectively, and suppose that ∂f and ∂g are α and β -cocoercive¹ operators, respectively, for some $\alpha \geq 0$ and $\beta \geq 0$. The problem is to*

$$\underset{x \in \mathcal{H}}{\text{minimize}} \quad f(x) + g(x), \quad (1)$$

under the assumption that its set of solutions S is nonempty.

Throughout this paper, 0-strongly convex functions, or functions with 0-cocoercive subdifferentials, are simply convex functions. This problem appears in several areas as variational mean field games [4, 5, 9, 10], optimal transport [4, 11, 22], image processing [7, 8, 23], among others.

[‡] DEPARTAMENTO DE MATEMÁTICA, UNIVERSIDAD TÉCNICA FEDERICO SANTA MARÍA, SANTIAGO, CHILE.
E-mail address: luis.briceno@usm.com.

[†]DEPARTAMENTO DE INGENIERÍA MATEMÁTICA, UNIVERSIDAD DE CONCEPCIÓN, CONCEPCIÓN, CHILE. *E-mail address:* fernandoroldan@udec.cl.

¹An operator $A: \mathcal{H} \rightarrow 2^{\mathcal{H}}$ is α -cocoercive for some $\alpha \geq 0$ if, for every $(x, y) \in \mathcal{H} \times \mathcal{H}$ and $(u, v) \in Ax \times Ay$, we have $\langle x - y \mid u - v \rangle \geq \alpha \|u - v\|^2$.

Problem 1.1 can be solved by the Douglas-Rachford splitting (DRS) [13] or the Peaceman–Rachford splitting (PRS) [24], the latter under an additional strong convexity or cocoercivity assumption on f or g [19]. Given $\tau > 0$ and $z_0 \in \mathcal{H}$, PRS iterates

$$(\forall n \in \mathbb{N}) \quad z_{n+1} = R_{\tau f} R_{\tau g} z_n, \quad (2)$$

where, for every $h \in \Gamma_0(\mathcal{H})$, $R_h = 2\text{prox}_h - \text{Id}$ is the reflected proximity operator of h , Id stands for the identity operator, and $\text{prox}_h: \mathcal{H} \rightarrow \mathcal{H}$ is the proximity operator of h , which associates to every $x \in \mathcal{H}$ the unique solution to the lower semicontinuous strongly convex problem

$$\underset{y \in \mathcal{H}}{\text{minimize}} \quad h(y) + \frac{1}{2} \|y - x\|^2. \quad (3)$$

In the general convex case, the operators $R_{\tau f}$ and $R_{\tau g}$ are nonexpansive, which is not enough to guarantee the weak convergence of a fixed point procedure of PRS. Indeed, by taking $\mathcal{H} = \mathbb{R}^2$ and f to be the indicator function of the x -axis and $g = 0$, it is clear that $R_{\tau g} = \text{Id}$, $R_{\tau f}$ is the reflection with respect to the x -axis, and PRS oscillates reflecting on the axis if the starting point is not on it (see, e.g., [21, Section 5.2]).

On the other hand, for some $\lambda \in]0, 1[$, DRS iterates

$$(\forall n \in \mathbb{N}) \quad z_{n+1} = (1 - \lambda)z_n + \lambda R_{\tau f} R_{\tau g} z_n, \quad (4)$$

which is a Krasnosel'skiĭ-Mann modification of PRS [14, 18, 20] achieving global weak convergence without additional assumptions [2, 25]². Note that PRS can be seen as a particular instance of (4) when $\lambda = 1$.

In the case when $\rho > 0$ and $\alpha > 0$, $R_{\tau f}$ is a strict contraction [16, Theorem 1], i.e., it satisfies

$$(\forall x \in \mathcal{H})(\forall y \in \mathcal{H}) \quad \|R_{\tau f}x - R_{\tau f}y\| \leq r(\tau)\|x - y\|, \quad (5)$$

where

$$r(\tau) = \max \left\{ \frac{\tau\alpha^{-1} - 1}{\tau\alpha^{-1} + 1}, \frac{1 - \tau\rho}{1 + \tau\rho} \right\} \in]0, 1[.$$

In this setting, PRS converges linearly with linear convergence rate $r(\tau)$, which is minimized when $\tau = \sqrt{\alpha/\rho}$, leading to the optimal linear convergence rate of $r^* = r(\sqrt{\alpha/\rho}) = \frac{1 - \sqrt{\alpha\rho}}{1 + \sqrt{\alpha\rho}}$. In the case when $\rho > 0$ and $\beta > 0$, i.e., when f is strongly convex and g is smooth, DRS converges linearly with an optimal rate $1/(1 + \sqrt{\beta\rho})$, which is achieved for $\tau = \sqrt{\alpha/\rho}$ and $\lambda = \frac{1 + \sqrt{\beta\rho}/2}{1 + \sqrt{\beta\rho}}$ [15, Theorem 5.6]. To the best of our knowledge, these are the best rates available in the literature for Problem 1.1 under strong convexity and smoothness for PRS and DRS. In [12], a review of the convergence rates for DRS and PRS are provided under various regularity assumptions, but the new derived linear convergence results are not valid for PRS. Of course, there exist alternative algorithms for solving Problem 1.1 under strong convexity and smoothness, as the gradient method or the proximal-gradient (or forward-backward) splitting, but their optimal rates and numerical performance are worse than that of PRS, as studied in [7, 8].

In this paper, we establish a sharp linear convergence rate for a new variant of PRS by optimally leveraging the strong convexity and smoothness properties of Problem 1.1 within a unified framework. The rate is obtained by adding and subtracting suitable quadratic terms from one function to the other so as to redistribute strong convexity in the primal formulation and smoothness in the dual formulation. We obtain an equivalent modified optimization problem in which each term has adjustable parameters of strong convexity and smoothness. By optimizing these parameters, we provide an optimal rate for general values of strong convexity and smoothness parameters in a novel algorithm obtained by applying PRS to the equivalent formulation. The optimal rate we obtain reduces to [16, Theorem 1] when $\mu = \beta = 0$, and is

²The classical DRS proposed in [13] is when $\lambda = 1/2$.

strictly lower than the optimal rates in [15, Theorem 5.6] when $\mu = \alpha = 0$ and in [6, Corollary 4.1] for FISTA under strong convexity. When strong convexity and/or smoothness appear in both functions, our approach provides an optimal balance of these properties leading to the best linear convergence rate in the literature. We finally provide some numerical experiments in an academic example and in two image processing problems to illustrate the advantages of our approach.

The paper is organized as follows. In Section 2 we present our notation and preliminary results. Our main results are provided in Section 3. Numerical experiments are studied in Section 4.

2. NOTATION AND PRELIMINARIES

Throughout this paper, \mathcal{H} is a real Hilbert space endowed with the inner product $\langle \cdot | \cdot \rangle$ and associated norm $\|\cdot\|$. Given a nonempty closed convex set $C \subset \mathcal{H}$, $\text{sri}(C)$ denotes its strong relative interior. Let $h: \mathcal{H} \rightarrow]-\infty, +\infty]$. The domain of h is $\text{dom } h = \{x \in \mathcal{H} \mid h(x) < +\infty\}$ and h is proper if $\text{dom } h \neq \emptyset$. Denote by $\Gamma_0(\mathcal{H})$ the class of proper lower semicontinuous convex functions from \mathcal{H} to $]-\infty, +\infty]$. Suppose that $h \in \Gamma_0(\mathcal{H})$. The subdifferential of h is the set-valued operator

$$\partial h: \mathcal{H} \rightarrow 2^{\mathcal{H}}: x \mapsto \{u \in \mathcal{H} \mid (\forall y \in \mathcal{H}) \quad \langle y - x \mid u \rangle + h(x) \leq h(y)\}, \quad (6)$$

which is maximally monotone, i.e., it is monotone

$$(\forall(x, y) \in (\text{dom } \partial h)^2)(\forall(u, v) \in \partial h(x) \times \partial h(y)) \quad \langle x - y \mid u - v \rangle \geq 0$$

and, if $B: \mathcal{H} \rightarrow 2^{\mathcal{H}}$ is a monotone operator such that $\text{gra } \partial h \subset \text{gra } B$, then $\partial h = B$, where $\text{dom } \partial h = \{x \in \mathcal{H} \mid \partial h(x) \neq \emptyset\}$ and $\text{gra } B = \{(x, u) \in \mathcal{H} \times \mathcal{H} \mid u \in Bx\}$. The Fenchel conjugate of h is

$$h^*: \mathcal{H} \rightarrow]-\infty, +\infty]: u \mapsto \sup_{x \in \mathcal{H}} (\langle x \mid u \rangle - h(x)). \quad (7)$$

We have $h^* \in \Gamma_0(\mathcal{H})$, $h^{**} = h$, and $(\partial h)^{-1} = \partial h^*$. Set $\rho \in [0, +\infty[$. We say that h is ρ -strongly convex if $h - \rho \|\cdot\|^2/2$ is convex. In particular, h is 0-strongly convex if and only if h is convex. Hence, it follows from [2, Example 22.4(iv)] that h is ρ -strongly convex then

$$(\forall(x, y) \in (\text{dom } \partial h)^2)(\forall(u, v) \in \partial h(x) \times \partial h(y)) \quad \langle x - y \mid u - v \rangle \geq \rho \|x - y\|^2. \quad (8)$$

Given $\alpha \geq 0$, ∂h is α -cocoercive if

$$(\forall(x, y) \in (\text{dom } \partial h)^2)(\forall(u, v) \in \partial h(x) \times \partial h(y)) \quad \langle x - y \mid u - v \rangle \geq \alpha \|u - v\|^2. \quad (9)$$

Note that, h is convex if and only if ∂h is 0-cocoercive. Moreover, if $\alpha > 0$ and $\text{dom } \partial h = \mathcal{H}$, the α -cocoercivity of ∂h implies the Gâteaux-differentiability of h [2, Propositions 16.27 & 17.31]. In addition, it follows from Cauchy-Schwarz inequality, that ∇h is α^{-1} -Lipschitz continuous, which implies the Fréchet differentiability of h [2, Corollary 17.42]. Actually, we have the following stronger result, which was first studied in [1].

Theorem 2.1. [2, Theorem 18.15] *Let $h: \mathcal{H} \rightarrow \mathbb{R}$ be continuous and convex and let $\alpha > 0$. The following are equivalent:*

- (1) h is Fréchet differentiable and ∇h is α^{-1} -Lipschitz continuous.
- (2) h is Fréchet differentiable and

$$(\forall x \in \mathcal{H})(\forall y \in \mathcal{H}) \quad \langle x - y \mid \nabla h(x) - \nabla h(y) \rangle \leq \alpha^{-1} \|x - y\|^2.$$

- (3) h is Fréchet differentiable and ∇h is α -cocoercive.
- (4) h^* is α -strongly convex.

The *proximity operator* of h is

$$\text{prox}_h : \mathcal{H} \rightarrow \mathcal{H} : x \mapsto \arg \min_{y \in \mathcal{H}} \left(h(y) + \frac{1}{2} \|x - y\|^2 \right), \quad (10)$$

which is characterized by

$$(\forall x \in \mathcal{H})(\forall p \in \mathcal{H}) \quad p = \text{prox}_h x \quad \Leftrightarrow \quad x - p \in \partial h(p) \quad (11)$$

and satisfies

$$(\forall \gamma \in]0, +\infty[) \quad \text{prox}_{\gamma h} = \text{Id} - \gamma \text{prox}_{h^*/\gamma} \circ (\text{Id} / \gamma), \quad (12)$$

where $\text{Id} : \mathcal{H} \rightarrow \mathcal{H}$ denotes the identity operator. The *reflected proximity operator* of h is

$$R_h = 2\text{prox}_h - \text{Id}.$$

In addition, we denote by $\text{Fix } T = \{x \in \mathcal{H} \mid x = Tx\}$ the set of fixed points of an operator $T : \mathcal{H} \rightarrow \mathcal{H}$. For further background on convex analysis, the reader is referred to [2].

3. MAIN RESULTS

Note that, in the context of Problem 1.1, it follows from Theorem 2.1 and Cauchy-Schwarz inequality that $\alpha\rho \in [0, 1]$ and $\beta\mu \in [0, 1]$. In the case when $\alpha\rho = 1$ and $\text{dom } \partial f = \mathcal{H}$, it follows from (8) and Theorem 2.1(2) that, for every $x \in \mathcal{H}$, $\langle \nabla f(x) \mid x \rangle = \rho\|x\|^2 + \langle \nabla f(0) \mid x \rangle$. Therefore, by integrating, we deduce

$$f(x) = f(0) + \langle \nabla f(0) \mid x \rangle + \frac{\rho}{2}\|x\|^2. \quad (13)$$

A similar quadratic form for g is obtained if $\beta\mu = 1$. These cases will be studied separately.

Definition 3.1. Given $h \in \Gamma_0(\mathcal{H})$ and $\delta \in \mathbb{R}$, we define $h_\delta = h + \frac{\delta}{2}\|\cdot\|^2$.

Proposition 3.2. Let $h \in \Gamma_0(\mathcal{H})$ be a ρ -strongly convex function such that ∂h is α -cocoercive, for some $\rho \geq 0$ and $\alpha \geq 0$ satisfying $\alpha\rho \in [0, 1]$. Then, the following hold:

(1) Suppose that $\alpha\rho = 1$ and $\text{dom } \partial h = \mathcal{H}$, and let $\delta \in [-\rho, +\infty[$. Then, there exists $a \in \mathbb{R}$ and $b \in \mathcal{H}$ such that

$$(h_\delta)^* = \begin{cases} \iota_{\{b\}} - a, & \text{if } \delta = -\rho; \\ \frac{\|\cdot - b\|^2}{2(\rho + \delta)} - a, & \text{if } \delta > -\rho \end{cases} \quad (14)$$

and, for every $\eta \in \mathbb{R}$,

$$(((h_\delta)^*)_\eta)^* = \begin{cases} \langle b \mid \cdot \rangle + a - \frac{\eta}{2}\|b\|^2, & \text{if } \delta = -\rho; \\ \iota_{\{-\frac{b}{\rho+\delta}\}} + a - \frac{\|b\|^2}{2(\rho+\delta)}, & \text{if } \delta > -\rho \text{ and } \eta = -\frac{1}{\rho+\delta}; \\ \frac{\|\cdot - \frac{b}{\rho+\delta}\|^2}{2(\eta + \frac{1}{\rho+\delta})} + a - \frac{\|b\|^2}{2(\rho+\delta)}, & \text{if } \delta > -\rho \text{ and } \eta > -\frac{1}{\rho+\delta}; \\ -\infty, & \text{otherwise.} \end{cases} \quad (15)$$

(2) Suppose that either $\alpha = 0$ or $\alpha > 0$ and $\text{dom } \partial h = \mathcal{H}$. Suppose that $\alpha\rho < 1$, let $\delta \in [-\rho, +\infty[$, and let $\eta \in [-\frac{\alpha}{1+\alpha\delta}, +\infty[$. Then, the following hold:

(a) $(h_\delta)^* \in \Gamma_0(\mathcal{H})$ and it is $\frac{\alpha}{1+\alpha\delta}$ -strongly convex.

(b) Suppose that $\delta > -\rho$. Then

(i) $\text{dom}(h_\delta)^* = \mathcal{H}$, $(h_\delta)^*$ is Fréchet differentiable and $\nabla(h_\delta)^*$ is $(\rho + \delta)$ -cocoercive.

(ii) $((h_\delta)^*)_\eta^* \in \Gamma_0(\mathcal{H})$ and it is $\frac{\rho + \delta}{1 + (\rho + \delta)\eta}$ -strongly convex.

(c) Suppose that $\eta > -\frac{\alpha}{1+\alpha\delta}$. Then $\text{dom}(((h_\delta)^*)_\eta)^* = \mathcal{H}$, $((h_\delta)^*)_\eta^*$ is Fréchet differentiable and $\nabla(((h_\delta)^*)_\eta)^*$ is $(\frac{\alpha}{1+\alpha\delta} + \eta)$ -cocoercive.

(3) For every $\tau \in]\max\{-\eta, 0\}, +\infty[$, suppose that $\delta(\tau + \eta) > -1$. Then

$$\text{prox}_{\tau(((h_\delta)^*)_\eta)^*} = \frac{\eta}{\tau + \eta} \text{Id} + \frac{\tau}{\tau + \eta} \text{prox}_{\frac{\tau + \eta}{1 + \delta(\tau + \eta)} h} \circ \left(\frac{\text{Id}}{1 + \delta(\tau + \eta)} \right) \quad (16)$$

and

$$R_{\tau(((h_\delta)^*)_\eta)^*} = \frac{2\tau}{\tau + \eta} \text{prox}_{\frac{\tau + \eta}{1 + \delta(\tau + \eta)} h} \circ \left(\frac{\text{Id}}{1 + \delta(\tau + \eta)} \right) - \frac{\tau - \eta}{\tau + \eta} \text{Id}. \quad (17)$$

Proof. Proof 1: It follows from (13) that $h_\delta = a + \langle b | \cdot \rangle + \frac{\rho + \delta}{2} \|\cdot\|^2$ for $a = h(0)$ and $b = \nabla h(0)$. The result follows from [2, Proposition 13.19 & Proposition 13.23] and straightforward computations. 2a: Since $h \in \Gamma_0(\mathcal{H})$ is ρ -strongly convex, $\phi := h - \frac{\rho}{2} \|\cdot\|^2$ is convex, thus, $h_\delta = \phi + (\rho + \delta) \|\cdot\|^2/2 \in \Gamma_0(\mathcal{H})$. Now, if $\alpha = 0$, the result is clear because 0-strongly convex functions are convex. If $\alpha > 0$ and $\text{dom } \partial h = \mathcal{H}$, it follows from Theorem 2.1 that h is Fréchet differentiable, ∇h is α^{-1} -Lipschitz continuous and, therefore, ∇h_δ is $(\alpha^{-1} + \delta)$ -Lipschitz continuous. The result follows from Theorem 2.1 now applied to h_δ . 2(b)i: If $\delta > -\rho$, h_δ is $(\rho + \delta)$ -strongly convex and the result is a consequence of Theorem 2.1. 2(b)ii : It follows from 2(b)i and 2a applied to $(h_\delta)^*$. 2c It follows directly by combining 2a and 2(b)i with the function $(h_\delta)^*$. 3: It follows from (12) and [2, Proposition 24.8(i)] that

$$\begin{aligned} \text{prox}_{\tau(((h_\delta)^*)_\eta)^*} &= \text{Id} - \tau \text{prox}_{((h_\delta)^*)_\eta / \tau} \circ \frac{\text{Id}}{\tau} \\ &= \text{Id} - \tau \text{prox}_{(h_\delta)^*/(\tau + \eta)} \circ \frac{\text{Id}}{\tau + \eta} \\ &= \text{Id} - \tau \left(\frac{\text{Id} - \text{prox}_{(\tau + \eta)h_\delta}}{\tau + \eta} \right) \\ &= \frac{\eta}{\tau + \eta} \text{Id} + \frac{\tau}{\tau + \eta} \text{prox}_{\frac{\tau + \eta}{1 + \delta(\tau + \eta)} h} \circ \frac{\text{Id}}{1 + \delta(\tau + \eta)}, \end{aligned} \quad (18)$$

and the result follows from $R_{\tau(((h_\delta)^*)_\eta)^*} = 2\text{prox}_{\tau(((h_\delta)^*)_\eta)^*} - \text{Id}$. \square

Proposition 3.3. In the context of Problem 1.1, suppose that $0 \in \text{sri}(\text{dom}(f) - \text{dom}(g))$, let $\delta \in [-\rho, \mu]$, let $\eta \in \left[-\frac{\alpha}{1 + \alpha\delta}, \frac{\beta}{1 - \beta\delta} \right]$, and consider the following optimization problem

$$\min_{x \in \mathcal{H}} (((f_\delta)^*)_\eta)^*(x) + (((g_{-\delta})^*)_{-\eta})^*(x), \quad (19)$$

where its solution set is denoted by \tilde{S} . Then, the following hold:

- (1) If $\eta = 0$, then $S = \tilde{S}$.
- (2) If $\eta > 0$, then $S = \text{prox}_{\frac{\eta}{1 + \eta\delta} f} \left(\frac{1}{1 + \eta\delta} \tilde{S} \right)$.
- (3) If $\eta < 0$, then $S = \text{prox}_{\frac{-\eta}{1 + \eta\delta} g} \left(\frac{1}{1 + \eta\delta} \tilde{S} \right)$.

Proof. Proof 1: If $\eta = 0$, since f_δ and $g_{-\delta}$ are in $\Gamma_0(\mathcal{H})$, we have $((f_\delta)^*)^* + ((g_{-\delta})^*)^* = f_\delta + g_{-\delta} = f + g$ and the result follows. 2: Let $x \in S$. Since $0 \in \text{sri}(\text{dom}(f) - \text{dom}(g))$, we deduce from [2, Theorem 16.3 & Corollary 16.48] that

$$\begin{aligned} x \in S &\Leftrightarrow 0 \in \partial f_\delta(x) + \partial g_{-\delta}(x) \\ &\Leftrightarrow (\exists u \in \mathcal{H}) \quad u \in \partial f_\delta(x) \quad \text{and} \quad -u \in \partial g_{-\delta}(x) \\ &\Leftrightarrow (\exists u \in \mathcal{H}) \quad x \in \partial(f_\delta)^*(u) \quad \text{and} \quad x \in \partial(g_{-\delta})^*(-u) \\ &\Leftrightarrow (\exists u \in \mathcal{H}) \quad x + \eta u \in \partial((f_\delta)^*)_\eta(u) \quad \text{and} \quad x + \eta u \in \partial((g_{-\delta})^*)_{-\eta}(-u) \end{aligned} \quad (20)$$

$$\Leftrightarrow (\exists u \in \mathcal{H}) \quad u \in \partial(((f_\delta)^*)_\eta)^*(x + \eta u) \quad \text{and} \quad -u \in \partial(((g_{-\delta})^*)_{-\eta})^*(x + \eta u), \quad (21)$$

which yields $z := x + \eta u \in \tilde{S}$ and, as a consequence, $\tilde{S} \neq \emptyset$. Hence, it follows from (20) and Definition 3.1 that

$$\frac{z - x}{\eta} \in \partial f_\delta(x) = \partial f(x) + \delta x \quad \Leftrightarrow \quad x = \text{prox}_{\frac{\eta}{1+\eta\delta} f} \left(\frac{z}{1+\eta\delta} \right) \quad (22)$$

and we conclude that $S \subset \text{prox}_{\frac{\eta}{1+\eta\delta} f} \left(\frac{1}{1+\eta\delta} \tilde{S} \right)$. Conversely, let $z \in \tilde{S}$ and $x = \text{prox}_{\frac{\eta}{1+\eta\delta} f} \left(\frac{z}{1+\eta\delta} \right)$. It follows from (22) that

$$u := \frac{z - x}{\eta} \in \partial f_\delta(x). \quad (23)$$

Now, since $\eta > 0 \geq -\frac{\alpha}{1+\alpha\delta}$, Proposition 3.2.2c asserts that $\text{dom}(((f_\delta)^*)_\eta)^* = \mathcal{H}$ and [2, Theorem 16.3 & Corollary 16.48] yield

$$\begin{aligned} z \in \tilde{S} &\Leftrightarrow 0 \in \partial(((f_\delta)^*)_\eta)^*(z) + \partial(((g_{-\delta})^*)_{-\eta})^*(z) \\ &\Leftrightarrow (\exists v \in \mathcal{H}) \quad -v \in \partial(((f_\delta)^*)_\eta)^*(z) \quad \text{and} \quad v \in \partial(((g_{-\delta})^*)_{-\eta})^*(z) \\ &\Leftrightarrow (\exists v \in \mathcal{H}) \quad z \in \partial(f_\delta)^*(-v) - \eta v \quad \text{and} \quad z \in \partial(g_{-\delta})^*(v) - \eta v \\ &\Leftrightarrow (\exists v \in \mathcal{H}) \quad -v \in \partial f_\delta(z + \eta v) \quad \text{and} \quad v \in \partial g_{-\delta}(z + \eta v) \quad (24) \\ &\Rightarrow (\exists v \in \mathcal{H}) \quad 0 \in \partial f(z + \eta v) + \partial g(z + \eta v) \\ &\Rightarrow (\exists v \in \mathcal{H}) \quad 0 \in \partial f(x + \eta(u + v)) + \partial g(x + \eta(u + v)). \quad (25) \end{aligned}$$

Moreover, since $z = x + \eta u$ in view of (23), it follows from (24) and the monotonicity of ∂f_δ that

$$0 \leq \langle u + v \mid -\eta(u + v) \rangle = -\eta \|u + v\|^2,$$

we conclude $u = -v$. Therefore, (25) implies $x \in S$. Finally, 3 is deduced analogously using $g_{-\delta}$ and $-\eta$ instead of f_δ and η . \square

Theorem 3.4. *In the context of Problem 1.1, suppose that $\max\{\alpha\rho, \beta\mu\} < 1$ and that $\min\{\rho + \mu, \alpha + \beta\} > 0$. Let $\delta \in [-\rho, \mu]$, $\eta \in \left[-\frac{\alpha}{1+\alpha\delta}, \frac{\beta}{1-\beta\delta} \right]$, and $\tau \in]|\eta|, +\infty[$ be such that $\tau|\delta| < 1 + \delta\eta$. Moreover, given $z_0 \in \mathcal{H}$, consider the recurrence*

$$\begin{aligned} &\text{For } n = 0, 1, 2, \dots \\ &\begin{cases} x_n = \text{prox}_{\frac{\tau+\eta}{1+\delta(\tau+\eta)} f} \left(\frac{z_n}{1 + \delta(\tau + \eta)} \right) \\ y_n = \frac{2\tau}{\tau+\eta} x_n - \frac{\tau-\eta}{\tau+\eta} z_n \\ p_n = \text{prox}_{\frac{\tau-\eta}{1-\delta(\tau-\eta)} g} \left(\frac{y_n}{1 - \delta(\tau - \eta)} \right) \\ z_{n+1} = z_n + \frac{2\tau}{\tau-\eta} (p_n - x_n). \end{cases} \quad (26) \end{aligned}$$

Then, the following hold:

(1) Set $\varphi_{\delta,\eta} := (((f_\delta)^*)_\eta)^*$ and $\psi_{\delta,\eta} := (((g_{-\delta})^*)_{-\eta})^*$. We have

$$\text{prox}_{\frac{\tau+\eta}{1+\delta(\tau+\eta)} f} \left(\frac{1}{1 + \delta(\tau + \eta)} \text{Fix}(R_{\tau\psi_{\delta,\eta}} \circ R_{\tau\varphi_{\delta,\eta}}) \right) = S \quad (27)$$

and there exist a unique $z^* \in \mathcal{H}$ such that $\text{Fix}(R_{\tau\psi_{\delta,\eta}} \circ R_{\tau\varphi_{\delta,\eta}}) = \{z^*\}$.

(2) $\{z_n\}_{n \in \mathbb{N}}$ converges linearly to z^* , i.e.,

$$(\forall n \in \mathbb{N}) \quad \|z_{n+1} - z^*\| \leq r(\tau, \eta, \delta) \|z_n - z^*\|,$$

where $r(\tau, \eta, \delta) = r_1(\tau, \eta, \delta)r_2(\tau, \eta, \delta) < 1$,

$$r_1(\tau, \eta, \delta) = \max \left\{ \frac{(\tau - \eta)(1 + \alpha\delta) - \alpha}{(\tau + \eta)(1 + \alpha\delta) + \alpha}, \frac{1 - (\tau - \eta)(\rho + \delta)}{1 + (\tau + \eta)(\rho + \delta)} \right\}, \quad (28)$$

and

$$r_2(\tau, \eta, \delta) = \max \left\{ \frac{(\tau + \eta)(1 - \beta\delta) - \beta}{(\tau - \eta)(1 - \beta\delta) + \beta}, \frac{1 - (\tau + \eta)(\mu - \delta)}{1 + (\tau - \eta)(\mu - \delta)} \right\}. \quad (29)$$

(3) The optimal convergence rate is

$$r^* = \frac{\sqrt{(1 + \beta\rho)(1 + \alpha\mu)} - \sqrt{(\alpha + \beta)(\rho + \mu)}}{\sqrt{(1 + \beta\rho)(1 + \alpha\mu)} + \sqrt{(\alpha + \beta)(\rho + \mu)}}, \quad (30)$$

which is achieved by taking

$$(\forall \delta \in [-\rho, \mu]) \quad \begin{cases} \eta(\delta) = \frac{\beta\rho - \alpha\mu + \delta(\alpha(1 + \beta\mu) + \beta(1 + \alpha\rho))}{(\rho + \delta)(\mu - \delta)(\alpha + \beta) + (1 + \alpha\delta)(1 - \beta\delta)(\rho + \mu)} \\ \tau(\delta) = \frac{\sqrt{(\alpha + \beta)(\rho + \mu)(1 + \alpha\mu)(1 + \beta\rho)}}{(\rho + \delta)(\mu - \delta)(\alpha + \beta) + (1 + \alpha\delta)(1 - \beta\delta)(\rho + \mu)}. \end{cases} \quad (31)$$

(4) The optimal rate r^* in (30) is tight, by taking $\mathcal{H} = \mathbb{R}^2$,

$$f: (x_1, x_2) \mapsto \frac{\rho}{2}x_1^2 + \frac{1}{2\alpha}x_2^2, \quad \text{and} \quad g: (x_1, x_2) \mapsto \frac{\mu}{2}x_1^2 + \frac{1}{2\beta}x_2^2. \quad (32)$$

Proof. Proof

1: We assert that

$$R_{\tau\varphi_{\delta,\eta}} \circ R_{\tau\psi_{\delta,\eta}} \text{ is } r(\tau, \eta, \delta)\text{-Lipschitz continuous with } r(\tau, \eta, \delta) < 1. \quad (33)$$

Hence, the Banach–Picard Theorem [2, Theorem 1.50] yields $\text{Fix}(R_{\tau\psi_{\delta,\eta}} \circ R_{\tau\varphi_{\delta,\eta}}) = \{z^*\}$ for some $z^* \in \mathcal{H}$. Indeed, first suppose that $\delta \in]-\rho, \mu[$. Since $\rho + \mu > 0$, it follows from Proposition 3.2(2b) that $\varphi_{\delta,\eta}$ is $\frac{\rho+\delta}{1+(\rho+\delta)\eta}$ -strongly convex and $\psi_{\delta,\eta}$ is $\frac{\mu-\delta}{1-(\mu-\delta)\eta}$ -strongly convex. Moreover, since $\eta \in]-\frac{\alpha}{1+\alpha\delta}, \frac{\beta}{1-\beta\delta}[$ and $\alpha + \beta > 0$, Proposition 3.2(2c) asserts that $\varphi_{\delta,\eta}$ and $\psi_{\delta,\eta}$ are Fréchet differentiable with full domain and their gradients are $(\frac{\alpha}{1+\alpha\delta} + \eta)$ - and $(\frac{\beta}{1-\beta\delta} - \eta)$ -cocoercive, respectively. Therefore, since (28) and (29) can be written equivalently as

$$\begin{aligned} r_1(\tau, \eta, \delta) &= \max \left\{ \frac{\frac{\tau}{1+\alpha\delta} + \eta - 1}{\frac{\tau}{1+\alpha\delta} + \eta + 1}, \frac{1 - \frac{\tau(\rho+\delta)}{1+(\rho+\delta)\eta}}{1 + \frac{\tau(\rho+\delta)}{1+(\rho+\delta)\eta}} \right\} \quad \text{and} \\ r_2(\tau, \eta, \delta) &= \max \left\{ \frac{\frac{\tau}{1-\beta\delta} - \eta - 1}{\frac{\tau}{1-\beta\delta} - \eta + 1}, \frac{1 - \frac{\tau(\mu-\delta)}{1-(\mu-\delta)\eta}}{1 + \frac{\tau(\mu-\delta)}{1-(\mu-\delta)\eta}} \right\}, \end{aligned} \quad (34)$$

it follows from [16, Theorem 1] that $R_{\tau\varphi_{\delta,\eta}}$ and $R_{\tau\psi_{\delta,\eta}}$ are $r_1(\tau, \eta, \delta)$ - and $r_2(\tau, \eta, \delta)$ -Lipschitz continuous, with $r_1(\tau, \eta, \delta) < 1$ and $r_2(\tau, \eta, \delta) < 1$ and (33) holds. In the case when $\delta = -\rho$, $R_{\tau\varphi_{\delta,\eta}}$ is merely nonexpansive in view of Proposition 3.2(2) and [2, Corollary 23.11]. However, as before, $R_{\tau\psi_{\delta,\eta}}$ is $r_2(\tau, \eta, \delta)$ -Lipschitz continuous with $r_2(\tau, \eta, \delta) < 1$, leading to the same conclusion. The case $\delta = \mu$ is analogous.

Now set $x^* = \text{prox}_{\frac{\tau+\eta}{1+\delta(\tau+\eta)} f} \left(\frac{z^*}{1+\delta(\tau+\eta)} \right)$, $y^* = R_{\tau\varphi_{\delta,\eta}} z^*$, and $p^* = \text{prox}_{\frac{\tau-\eta}{1-\delta(\tau-\eta)} g} \left(\frac{y^*}{1-\delta(\tau-\eta)} \right)$. Then, it follows from Proposition 3.2(3) that

$$y^* = \frac{2\tau}{\tau+\eta} x^* - \frac{\tau-\eta}{\tau+\eta} z^*, \quad (35)$$

which yields

$$\begin{aligned} z^* = R_{\tau\psi_{\delta,\eta}} \circ R_{\tau\varphi_{\delta,\eta}} z^* &\Leftrightarrow z^* = \frac{2\tau}{\tau-\eta} p^* - \frac{\tau+\eta}{\tau-\eta} y^* \\ &\Leftrightarrow z^* = \frac{2\tau}{\tau-\eta} p^* - \frac{\tau+\eta}{\tau-\eta} \left(\frac{2\tau}{\tau+\eta} x^* - \frac{\tau-\eta}{\tau+\eta} z^* \right) \\ &\Leftrightarrow x^* = p^*. \end{aligned}$$

Hence, since

$$\frac{z^* - (1 + \delta(\tau + \eta))x^*}{\tau + \eta} \in \partial f(x^*) \quad \text{and} \quad \frac{y^* - (1 - \delta(\tau - \eta))x^*}{\tau - \eta} \in \partial g(p^*) = \partial g(x^*)$$

and, in view of (35),

$$\frac{z^* - (1 + \delta(\tau + \eta))x^*}{\tau + \eta} + \frac{y^* - (1 - \delta(\tau - \eta))x^*}{\tau - \eta} = \frac{1}{\tau - \eta} \left(\frac{\tau - \eta}{\tau + \eta} z^* + y^* - \frac{2\tau}{\tau + \eta} x^* \right) = 0.$$

Therefore, we conclude that $0 \in \partial f(x^*) + \partial g(x^*)$ and $x^* \in S$ in view of [2, Theorem 16.3]. The result follows from the strict convexity of $f + g$ and [2, Corollary 11.9].

2: It follows from Proposition 3.2(3) that

$$R_{\tau\varphi_{\delta,\eta}} = \frac{2\tau}{\tau + \eta} \text{prox}_{\frac{\tau+\eta}{1+\delta(\tau+\eta)} f} \circ \left(\frac{\text{Id}}{1 + \delta(\tau + \eta)} \right) - \frac{\tau - \eta}{\tau + \eta} \text{Id} \quad (36)$$

and

$$R_{\tau\psi_{\delta,\eta}} = \frac{2\tau}{\tau - \eta} \text{prox}_{\frac{\tau-\eta}{1-\delta(\tau-\eta)} g} \circ \left(\frac{\text{Id}}{1 - \delta(\tau - \eta)} \right) - \frac{\tau + \eta}{\tau - \eta} \text{Id} \quad (37)$$

Hence, it follows from (26) that, for every $n \in \mathbb{N}$, $y_n = R_{\tau\varphi_{\delta,\eta}} z_n$ and

$$\begin{aligned} (\forall n \in \mathbb{N}) \quad z_{n+1} &= z_n + \frac{2\tau}{\tau - \eta} \left[\text{prox}_{\frac{\tau-\eta}{1-\delta(\tau-\eta)} g} \left(\frac{y_n}{1 - \delta(\tau - \eta)} \right) - \text{prox}_{\frac{\tau+\eta}{1+\delta(\tau+\eta)} f} \left(\frac{z_n}{1 + \delta(\tau + \eta)} \right) \right] \\ &= \frac{2\tau}{\tau - \eta} \text{prox}_{\frac{\tau-\eta}{1-\delta(\tau-\eta)} g} \left(\frac{y_n}{1 - \delta(\tau - \eta)} \right) - \frac{\tau + \eta}{\tau - \eta} y_n \\ &= R_{\tau\psi_{\delta,\eta}} R_{\tau\varphi_{\delta,\eta}} z_n. \end{aligned} \quad (38)$$

Then, the linear convergence follows from (33).

3: Note that, given $\delta \in] - \rho, \mu [$ and $\eta \in] - \frac{\alpha}{1+\alpha\delta}, \frac{\beta}{1-\beta\delta} [$, by defining

$$\phi_1: \tau \mapsto \frac{(\tau - \eta)(1 + \alpha\delta) - \alpha}{(\tau + \eta)(1 + \alpha\delta) + \alpha} \quad \text{and} \quad \phi_2: \tau \mapsto \frac{1 - (\tau - \eta)(\rho + \delta)}{1 + (\tau + \eta)(\rho + \delta)}, \quad (39)$$

which are strictly increasing and strictly decreasing, respectively, $r_1(\cdot, \eta, \delta)$ is minimized at $\tau_1(\eta, \delta) > 0$ satisfying $\phi_1(\tau_1(\eta, \delta)) = \phi_2(\tau_1(\eta, \delta))$ or, equivalently,

$$\tau_1(\eta, \delta) = \sqrt{\frac{\alpha}{1 + \alpha\delta} + \eta} \sqrt{\frac{1}{\rho + \delta} + \eta}. \quad (40)$$

We deduce

$$r_1(\tau_1(\eta, \delta), \eta, \delta) = \frac{\sqrt{\frac{\frac{1}{\rho+\delta}+\eta}{\frac{\alpha}{1+\alpha\delta}+\eta}} - 1}{\sqrt{\frac{\frac{1}{\rho+\delta}+\eta}{\frac{\alpha}{1+\alpha\delta}+\eta}} + 1}. \quad (41)$$

Analogously, $r_2(\cdot, \eta, \delta)$ is minimized at $\tau_2(\eta, \delta) > 0$ satisfying

$$\tau_2(\eta, \delta) = \sqrt{\frac{\beta}{1-\beta\delta}} - \eta \sqrt{\frac{1}{\mu-\delta} - \eta} \quad (42)$$

and

$$r_2(\tau_2(\eta, \delta), \eta, \delta) = \frac{\sqrt{\frac{\frac{1}{\mu-\delta}-\eta}{\frac{\beta}{1-\beta\delta}-\eta}} - 1}{\sqrt{\frac{\frac{1}{\mu-\delta}-\eta}{\frac{\beta}{1-\beta\delta}-\eta}} + 1}. \quad (43)$$

Therefore, $r(\cdot, \eta, \delta)$ is minimized at $\tau_1(\eta, \delta) = \tau_2(\eta, \delta)$, which is equivalent to

$$\eta = \frac{\frac{\beta}{(1-\beta\delta)(\mu-\delta)} - \frac{\alpha}{(1+\alpha\delta)(\rho+\delta)}}{\frac{\alpha}{1+\alpha\delta} + \frac{1}{\rho+\delta} + \frac{\beta}{1-\beta\delta} + \frac{1}{\mu-\delta}} =: \eta(\delta) \quad (44)$$

and

$$r(\tau_1(\eta, \delta), \eta, \delta) = \left(\frac{\sqrt{\frac{\frac{1}{\rho+\delta}+\eta}{\frac{\alpha}{1+\alpha\delta}+\eta}} - 1}{\sqrt{\frac{\frac{1}{\rho+\delta}+\eta}{\frac{\alpha}{1+\alpha\delta}+\eta}} + 1} \right) \left(\frac{\sqrt{\frac{\frac{1}{\mu-\delta}-\eta}{\frac{\beta}{1-\beta\delta}-\eta}} - 1}{\sqrt{\frac{\frac{1}{\mu-\delta}-\eta}{\frac{\beta}{1-\beta\delta}-\eta}} + 1} \right). \quad (45)$$

By replacing (44) in (45), we obtain

$$r(\delta) = \left(\frac{\sqrt{\frac{(1+\beta\rho)(\rho+\mu)}{(1+\alpha\mu)(\alpha+\beta)}} \left(\frac{1+\alpha\delta}{\rho+\delta} \right) - 1}{\sqrt{\frac{(1+\beta\rho)(\rho+\mu)}{(1+\alpha\mu)(\alpha+\beta)}} \left(\frac{1+\alpha\delta}{\rho+\delta} \right) + 1} \right) \left(\frac{\sqrt{\frac{(1+\alpha\mu)(\rho+\mu)}{(1+\beta\rho)(\alpha+\beta)}} \left(\frac{1-\beta\delta}{\mu-\delta} \right) - 1}{\sqrt{\frac{(1+\alpha\mu)(\rho+\mu)}{(1+\beta\rho)(\alpha+\beta)}} \left(\frac{1-\beta\delta}{\mu-\delta} \right) + 1} \right), \quad (46)$$

which turns out to be constant (see Appendix), more precisely,

$$(\forall \delta \in [-\rho, \mu]) \quad r(\delta) = r^* = \frac{\sqrt{(1+\beta\rho)(1+\alpha\mu)} - \sqrt{(\alpha+\beta)(\rho+\mu)}}{\sqrt{(1+\beta\rho)(1+\alpha\mu)} + \sqrt{(\alpha+\beta)(\rho+\mu)}}. \quad (47)$$

Moreover, by using (44) in (42), we deduce $\tau_2(\eta(\delta), \delta) = \tau(\delta)$ defined in (31).

On the other hand, if $\delta = \mu$, since $r_2(\tau, \eta, \mu) = 1$, the argument is simpler and leads to the same constant. In this case it is only necessary to minimize r_1 , which leads to an optimal $\tau_1(\eta, \mu)$ defined in (40) and an optimal value $r_1(\tau_1(\eta, \mu), \eta, \mu)$ defined in (41). Since $\eta \mapsto r_1(\tau_1(\eta, \mu), \eta, \mu)$ is decreasing, its minimal value is obtained when $\eta_1 = \frac{\beta}{1-\beta\mu}$, which yields $r^* = r_1(\tau_1(\eta_1, \mu), \eta_1, \mu)$ and that

$$\tau_1(\eta_1, \mu) = \frac{1}{1-\beta\mu} \sqrt{\frac{(1+\beta\rho)(\alpha+\beta)}{(1+\alpha\mu)(\rho+\mu)}} = \tau(\mu). \quad (48)$$

The case $\delta = -\rho$ leads to $r_1(\tau, \eta, \mu) = 1$ and the argument is analogous.

4: It follows from (32) and straightforward computations that

$$(\forall \gamma > 0) \quad \begin{cases} \text{prox}_{\gamma f}: (x_1, x_2) \mapsto \left(\frac{x_1}{1+\gamma\rho}, \frac{x_2}{1+\gamma/\alpha} \right), \\ \text{prox}_{\gamma g}: (x_1, x_2) \mapsto \left(\frac{x_1}{1+\gamma\mu}, \frac{x_2}{1+\gamma/\beta} \right). \end{cases} \quad (49)$$

Then, let $\delta \in [-\rho, \mu]$ and let $\eta = \eta(\delta)$ and $\tau = \tau(\delta)$ defined in (31), it follows from Proposition 3.2(3) that

$$\begin{cases} R_{\tau\varphi_{\delta,\eta}} : (x_1, x_2) \mapsto \left(\left(\frac{1+(\eta-\tau)(\rho+\delta)}{1+(\eta+\tau)(\rho+\delta)} \right) x_1, - \left(\frac{(\tau-\eta)(1+\alpha\delta)-\alpha}{(\tau+\eta)(1+\alpha\delta)+\alpha} \right) x_2 \right), \\ R_{\tau\psi_{\delta,\eta}} : (x_1, x_2) \mapsto \left(\left(\frac{1-(\tau+\eta)(\mu-\delta)}{1+(\tau-\eta)(\mu-\delta)} \right) x_1, - \left(\frac{(\tau+\eta)(1-\beta\delta)-\beta}{(\tau-\eta)(1-\beta\delta)+\beta} \right) x_2 \right). \end{cases} \quad (50)$$

Hence, by recalling that (26) is equivalent to (38) and that $\tau = \tau_1(\eta, \delta)$ is chosen for guaranteeing that $\phi_1(\tau_1(\eta, \delta)) = \phi_2(\tau_1(\eta, \delta))$ and η for obtaining $\tau = \tau_1(\eta, \delta) = \tau_2(\eta, \delta)$ (see (40) and (42)), we deduce

$$(\forall n \in \mathbb{N}) \quad \begin{cases} z_{n+1}^1 = \left(\frac{1-(\tau-\eta)(\rho+\delta)}{1+(\tau+\eta)(\rho+\delta)} \right) \left(\frac{1-(\tau+\eta)(\mu-\delta)}{1+(\tau-\eta)(\mu-\delta)} \right) z_n^1 = r^* z_n^1 \\ z_{n+1}^2 = \left(\frac{(\tau-\eta)(1+\alpha\delta)-\alpha}{(\tau+\eta)(1+\alpha\delta)+\alpha} \right) \left(\frac{(\tau+\eta)(1-\beta\delta)-\beta}{(\tau-\eta)(1-\beta\delta)+\beta} \right) z_n^2 = r^* z_n^2. \end{cases} \quad (51)$$

Moreover, since $z^* = (0, 0)$, we deduce that $\|z_{n+1} - z^*\| = r^* \|z_n - z^*\|$ and the result follows. \square

Remark 3.5. (1) Note that the optimal rate obtained in Theorem 3.4 is lower than the two possible rates derived from [16, Proposition 3]. Indeed, noting that $x \mapsto \frac{1-x}{1+x}$ is strictly decreasing and $\frac{(\alpha+\beta)(\rho+\mu)}{(1+\alpha\mu)(1+\beta\rho)} \geq \max\{\alpha\rho, \beta\mu\}$, we have

$$r^* = \frac{1 - \sqrt{\frac{(\alpha+\beta)(\rho+\mu)}{(1+\alpha\mu)(1+\beta\rho)}}}{1 + \sqrt{\frac{(\alpha+\beta)(\rho+\mu)}{(1+\alpha\mu)(1+\beta\rho)}}} \leq \min \left\{ \frac{1 - \sqrt{\alpha\rho}}{1 + \sqrt{\alpha\rho}}, \frac{1 - \sqrt{\beta\mu}}{1 + \sqrt{\beta\mu}} \right\} \quad (52)$$

and the inequality is strict because $\max\{\alpha\rho, \beta\mu\} < 1$ and $\min\{\rho + \mu, \alpha + \beta\} > 0$.

(2) The optimal rate obtained in Theorem 3.4 is lower than the rate of convergence obtained for FISTA in [6, Corollary 4.1]. Indeed, since, $\frac{(\alpha+\beta)(\rho+\mu)}{(1+\alpha\mu)(1+\beta\rho)} \geq \max \left\{ \frac{\alpha(\rho+\mu)}{1+\alpha\mu}, \frac{\beta(\rho+\mu)}{1+\beta\rho} \right\}$, we deduce

$$r^* \leq \min \left\{ \frac{1 - \sqrt{\frac{\alpha(\rho+\mu)}{1+\alpha\mu}}}{1 + \sqrt{\frac{\alpha(\rho+\mu)}{1+\alpha\mu}}}, \frac{1 - \sqrt{\frac{\beta(\rho+\mu)}{1+\beta\rho}}}{1 + \sqrt{\frac{\beta(\rho+\mu)}{1+\beta\rho}}} \right\} \leq \min \left\{ 1 - \sqrt{\frac{\alpha(\rho+\mu)}{1+\alpha\mu}}, 1 - \sqrt{\frac{\beta(\rho+\mu)}{1+\beta\rho}} \right\}$$

and the inequality is strict because $\max\{\alpha\rho, \beta\mu\} < 1$ and $\min\{\rho + \mu, \alpha + \beta\} > 0$.

(3) In the particular case when $\rho > 0$, $\beta > 0$, and $\alpha = \mu = 0$, the optimal rate obtained in Theorem 3.4 reduces to

$$r^* = \frac{\sqrt{1+\beta\rho} - \sqrt{\beta\rho}}{\sqrt{1+\beta\rho} + \sqrt{\beta\rho}} \quad (53)$$

which is strictly lower than the bound obtained in [15, Theorem 5.6], when $B = \partial g$ is β -cocoercive and $A = \partial f$ is ρ -strongly monotone, which is $\frac{1}{1+\sqrt{\beta\rho}}$. Hence, r^* is the best convergence rate available in the literature for Peaceman–Rachford for minimizing Problem 1.1 when f is ρ -strongly convex and ∇g is β^{-1} -Lipschitz continuous.

(4) A simple choice of parameters achieving the optimal convergence rate is to consider

$$\delta^* = \frac{\alpha\mu - \beta\rho}{\beta(1+\alpha\mu) + \alpha(1+\beta\rho)} \in]-\rho, \mu[, \quad (54)$$

which leads $\eta^* = 0$ in (44) and, from (40) (or (42))

$$\tau^* = \frac{\beta(1+\alpha\mu) + \alpha(1+\beta\rho)}{\sqrt{(\alpha+\beta)(\rho+\mu)(1+\alpha\mu)(1+\beta\rho)}}. \quad (55)$$

In this case, the algorithm in (26) reduces to

$$(\forall n \in \mathbb{N}) \quad \begin{cases} x_n = \text{prox}_{\frac{\tau^*}{1+\delta^*\tau^*}f} \left(\frac{z_n}{1+\delta^*\tau^*} \right) \\ y_n = 2x_n - z_n \\ p_n = \text{prox}_{\frac{\tau^*}{1-\delta^*\tau^*}g} \left(\frac{y_n}{1-\delta^*\tau^*} \right) \\ z_{n+1} = z_n + 2(p_n - x_n). \end{cases} \quad (56)$$

4. NUMERICAL EXPERIMENTS

In this section, we present numerical experiments to illustrate the advantages of our approach. First, we introduce an academic example and then we provide some applications to image processing.

4.1. Academic Example. Consider Problem 1.1 in the case when $\mathcal{H} = \mathbb{R}^m$,

$$f: x \mapsto \frac{1}{2}\|Ax - a\|^2, \quad \text{and} \quad g: x \mapsto \frac{1}{2}\|Bx - b\|^2, \quad (57)$$

where A and B are non-zero $n \times m$ and $p \times m$ real matrices, respectively, $a \in \mathbb{R}^n$, and $b \in \mathbb{R}^p$. Note that, since $\nabla f: x \mapsto A^\top(Ax - a)$ and $\nabla g: x \mapsto B^\top(Bx - b)$ are $\|A\|^2$ - and $\|B\|^2$ -Lipschitz continuous, then $\alpha = 1/\|A\|^2 > 0$ and $\beta = 1/\|B\|^2 > 0$ in view of Theorem 2.1. The strong convexity of f (resp. g) with $\rho > 0$ (resp. $\mu > 0$) is guaranteed when A (resp. B) is injective, which is only possible if $m \leq n$ (resp. $m \leq p$). In this setting, the strong convexity parameter of f and g corresponds to $\lambda_{\min}(A^\top A)$ and $\lambda_{\min}(B^\top B)$ ³, respectively.

In the numerical experiment below, we consider 10 different dimension configurations for (m, n, p) detailed in Table 1 and, for each one, we generate 30 random instances for matrices A and B , generated in Julia by considering $A = 0.5 \cdot \text{rand}(m, n)$ and $B = 15 \cdot \text{rand}(m, p)$, where the function $\text{rand}(m, n)$ generates a dense $m \times n$ matrix with independent random numbers uniformly distributed in $[0, 1]$. We first compare with the average number of iterations and computational time to achieve $\|z_k - z^*\| \leq tol = 10^{-10}$ for the classical PRS when either f or g are strongly convex by using the optimal step-size derived in [16, Proposition 3]. We call PRS1 to PRS with optimal step-size when f is strongly convex and PRS2 when g is. Note that in the cases when $m > n$ (resp. $m > p$), PRS1 (resp. PRS2) cannot be implemented because $\rho = 0$ (resp. $\mu = 0$), in view of [16, Proposition 3]. In Table 1 we observe an important reduction in the number of iterations and computational time except for the dimensions $(20, 20, 10)$ and $(40, 40, 20)$, in which the performances of PRS lev and PRS1 are very similar. In this case, note that the strong convexity of the problem is not relevant and the average values of the parameters lead to $r^* = 0.990604$, which is very close to 1 and the optimal rate in [16, Proposition 3] is 0.990615. When the strong convexity is more important we can observe a reduction in the average of iterations up to 96.5%. In Figure 1 we show a plot of the error versus iterations for a choice of particular instances in each dimension.

4.2. Image processing. Let $(n_1, n_2, m_1, m_2) \in \mathbb{N}^4$ and let $x \in \mathbb{R}^{n_1 \times n_2}$ be an image to be recovered from an observation

$$b = Tx + \epsilon, \quad (58)$$

where $T: \mathbb{R}^{n_1 \times n_2} \rightarrow \mathbb{R}^{m_1 \times m_2}$ is an operator representing the observation process and ϵ is an additive noise. The original image x can be approximated by solving Problem 1.1 by setting $\mathcal{H} = \mathbb{R}^{n \times n}$,

$$f: x \mapsto \frac{1}{2}\|Tx - b\|^2, \quad \text{and} \quad g: x \mapsto \lambda H^\varepsilon(Wx), \quad (59)$$

³Given a symmetric matrix D , $\lambda_{\min}(D)$ denotes the lowest real eigenvalue of D .

(m, n, p)	PRS lev				PRS 1		PRS 2			
	avg ρ	avg α	avg μ	avg β	Iter.	Time (ms)	Iter.	Time (ms)	Iter.	Time (ms)
(20, 10, 20)	0.0	0.077	0.883	4.2e-5	91.4	1.14	-	-	1396.9	20.4
(20, 20, 10)	5.7e-4	0.039	0.0	8.4e-5	1875.4	25.7	1874.0	25.7	-	-
(20, 20, 20)	5.7e-4	0.039	0.883	4.2e-5	130.5	1.85	5179.8	71.0	1029.0	13.6
(20, 40, 20)	0.105	0.020	0.883	4.2e-5	107.2	1.48	252.8	3.43	688.0	9.5
(20, 20, 40)	5.7e-4	0.039	87.3	2.2e-5	8.6	0.19	5317.5	71.8	237.1	3.5
(40, 20, 40)	0.0	0.020	0.264	1.1e-5	745.3	34.3	-	-	2093.3	78.07
(40, 40, 20)	3.7e-4	9.8e-3	0.0	2.2e-5	3981.2	145.2	3978.6	144.7	-	-
(40, 40, 40)	3.7e-4	9.8e-3	0.264	1.1e-5	893.2	34.3	7683.7	289.7	1119.6	42.1
(40, 80, 40)	0.189	4.9e-3	0.264	1.1e-5	278.7	11.46	377.5	15.6	634.7	26.4
(40, 40, 80)	3.7e-4	9.8e-3	153.9	5.5e-6	11.6	0.91	7856.5	515.6	340.1	19.2

TABLE 1. Average parameters, number of iterations and computational time (ms) for PRS lev, PRS 1, and PRS 2 to reach a tolerance of $\|z_k - z^*\| < 10^{-10}$ in 30 random instances of A and B with $a, b = 0$, $tol = 10^{-10}$.

where $\lambda \in]0, +\infty[$ is a regularization parameter, $H^\varepsilon : \mathbb{R}^{n_1 \times n_2} \rightarrow \mathbb{R}$ is the Huber function defined by

$$\left(\forall w = (\omega_{i,j})_{\substack{1 \leq i \leq n_1 \\ 1 \leq j \leq n_2}} \in \mathbb{R}^{n_1 \times n_2} \right) \quad H^\varepsilon(w) = \sum_{i=1}^{n_1} \sum_{j=1}^{n_2} h^\varepsilon(\omega_{i,j}), \quad (60)$$

and

$$(\forall \xi \in \mathbb{R}) \quad h^\varepsilon(\xi) = \begin{cases} |\xi| - \frac{\varepsilon}{2}, & \text{if } |\xi| > \varepsilon, \\ \frac{\xi^2}{2\varepsilon}, & \text{otherwise.} \end{cases} \quad (61)$$

and $W : \mathbb{R}^{n_1 \times n_2} \rightarrow \mathbb{R}^{n_1 \times n_2}$ is an orthogonal basis wavelet transform. Note that f is $\lambda_{\min}(T^\top T)$ -strongly convex, ∇f is $\|T\|^2$ -Lipschitz continuous, g is convex and $\nabla g = \lambda W^\top \nabla H^\varepsilon W$ is λ/ε -Lipschitz continuous. Thus, in the context of Problem 1.1, we have $\rho = \lambda_{\min}(T^\top T)$, $\alpha = \|T\|^{-2}$, $\mu = 0$, and $\beta = \varepsilon/\lambda$. We solve this problem using our approach, PRS with the optimal step-size in [16, Proposition 3], and FISTA in its leveraged form for strongly convex problems [3, 6]. Note that we can apply FISTA either with a backward step in g and a forward step in f , or vice versa, which are called by FISTA 1 and FISTA 2, respectively.

We consider the scenarios where T is a blur operator in image restoration and where T is the discrete Radon transform in computed tomography (CT) [17]. In each experiment, we use a stopping criterion consisting of a maximum of 10^3 iterations and a *normalized error* with a tolerance of 10^{-12} , i.e., given a solution z^* , the algorithm stops if

$$\frac{\|z_{n+1} - z^*\|}{\|z_0 - z^*\|} < 10^{-12}.$$

4.2.1. Image Restoration. In this case, T is a Gaussian point spread function of size 5×5 and standard deviation $\sigma \in]0, +\infty[$ and ϵ is a zero mean Gaussian noise with variance 0.008. We set $\varepsilon = 0.01$ and $\lambda = 0.07$. The operator W is a level-3 Haar basis wavelet transform. As a test image, we use the 512×512 image shown in Figure 3a. To test different values of ρ , we consider $\sigma \in \{0.5, 0.6\}$ which yield the values of ρ described in Table 2. This table also presents the results of our experiments. Note that PRS lev achieves better performance in terms of iteration number and CPU time in all cases when compared with PRS and the two versions of FISTA. Although its advantage over PRS is slight, Figure 2 illustrates both the theoretical and experimental benefits of the improved convergence rate of PRS lev in this case. The blurred

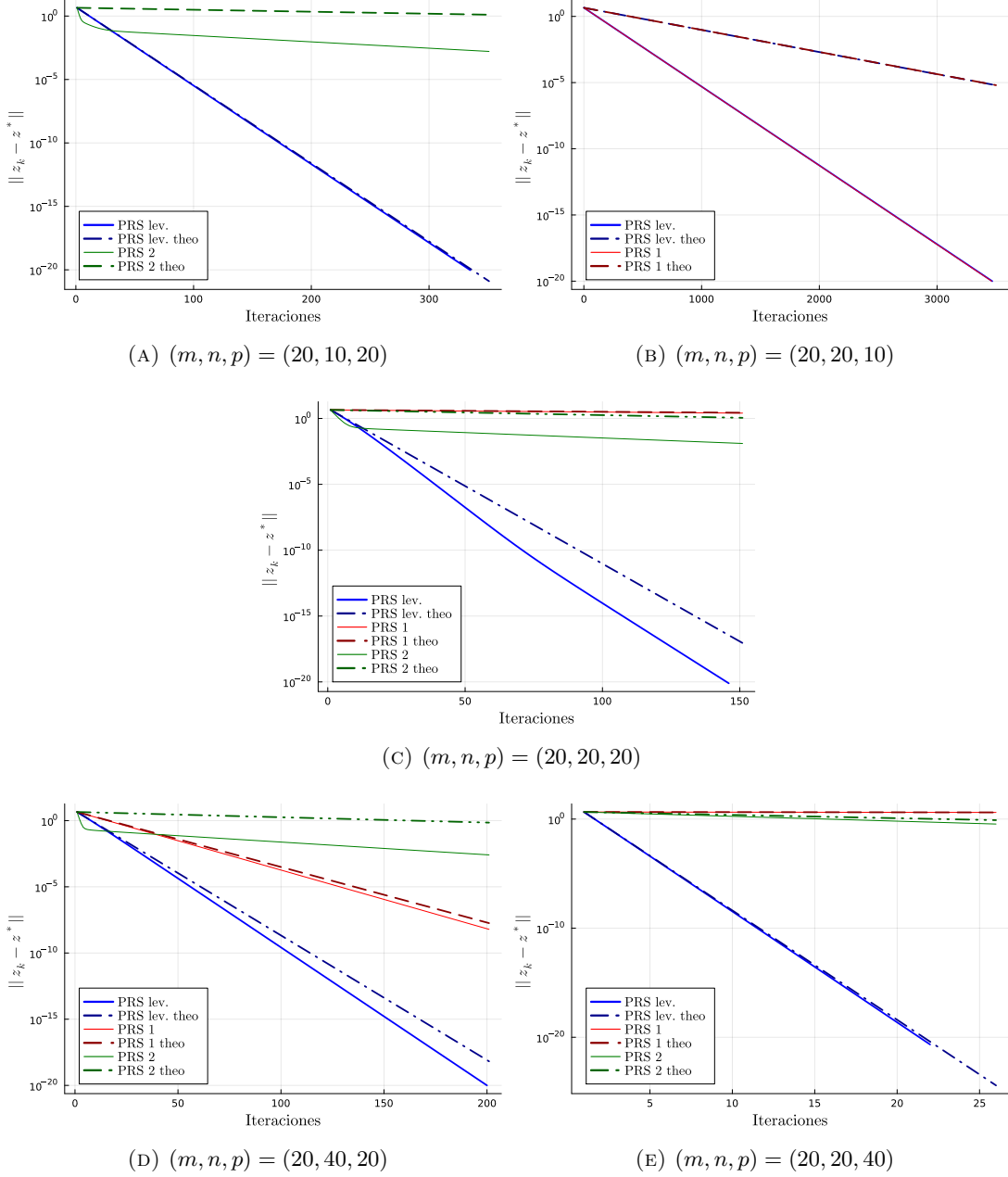


FIGURE 1. Theoretical bounds and numerical errors for random instances in different dimensions.

and noisy image, as well as the denoised results for each case, are shown in Figures 4 and 5, respectively.

4.2.2. Computed Tomography. Here T is the discretized Radon projector given by the line length ray-driven projector [28]. It was implemented in MATLAB using the line fan-beam

σ	ρ	α	μ	β	PRS lev		PRS		FISTA 1		FISTA 2	
					Iter.	Time (s)	Iter.	Time (s)	Iter.	Time (s)	Iter.	Time (s)
0.5	0.11	1	0	0.1429	39	1.38	42	1.54	59	2.06	189	6.93
0.6	0.013	1	0	0.1429	114	4.04	122	4.43	167	5.77	517	18.36

TABLE 2. Results in terms of number of iterations and CPU time in second.
We consider $tol = 10^{-12}$, $niter = 1000$

projector provided by the ASTRA toolbox [26, 27] with a fan-beam geometry over 180° , the source to object distance is 800 mm, and the source-to-image distance is 1200 mm. The test image x is created by the *phantom* function in MATLAB and we considered $n_1 = n_2 = n \in \{64, 128\}$. When $n = 64$, we consider 150 projection angles and a detector with 249 bins, for $n = 128$, we consider 360 projection angles and a detector with 249 bins, which results in sinograms of size $(m_1, m_2) = (112, 150)$ and $(m_1, m_2) = (249, 360)$, respectively. Moreover, we consider $\varepsilon = \lambda = 10^{-5}$ and W as an orthonormal Symmlet basis wavelet transform of level 2. The values of ρ , α , and β , for each case, are described in Table 3. To implement PRS lev, PRS, and FISTA 2, we calculate prox_f using the MATLAB function *inv* once outside the iterative scheme (the time required for this computation is included in the total running time of each algorithm). From Table 3 we observe that, in each case, PRS lev. exhibits the best overall performance. Note that PRS and FISTA reach the maximum number of iterations. Although FISTA 2 is competitive with PRS lev., Figure 6 shows that it is initially fast but subsequently follows its theoretical convergence rate, which is slower than that of PRS lev. The blurred and noisy image, along with the denoised reconstructions for each case, are displayed in Figures 7 and 8, respectively. We also observe that the reconstructions produced by PRS and FISTA 1 remain far from the target solution.

n	ρ	α	μ	β	PRS lev		PRS		FISTA 1		FISTA 2	
					Iter.	Time (s)	Iter.	Time (s)	Iter.	Time (s)	Iter.	Time (s)
64	0.0128	$5.6 \cdot 10^{-5}$	0	1	124	1.31	1000	5.24	1000	12.47	145	1.44
128	0.0026	$1.13 \cdot 10^{-5}$	0	1	274	27.0	1000	51.51	1000	189.0	334	31.0

TABLE 3. Results in terms of number of iterations and CPU time in second.
We consider $tol = 10^{-12}$, $niter = 1000$.

5. APPENDIX: PROOF OF $r(\delta)$ CONSTANT IN THEOREM 3.4

Proof. Proof Note that $r(\delta)$ defined in (46) can be written as $r(\delta) = \frac{N(\delta)}{D(\delta)}$, where

$$\begin{aligned} N(\delta) &= (ab(1 + \alpha\delta) - cd(\rho + \delta))(bc(1 - \beta\delta) - ad(\mu - \delta)) \\ D(\delta) &= (ab(1 + \alpha\delta) + cd(\rho + \delta))(bc(1 - \beta\delta) + ad(\mu - \delta)), \end{aligned} \quad (62)$$

and

$$\begin{aligned} a &= \sqrt{1 + \beta\rho}, \quad b = \sqrt{\rho + \mu}, \\ c &= \sqrt{1 + \alpha\mu}, \quad d = \sqrt{\alpha + \beta}. \end{aligned} \quad (63)$$

Then, by setting $A_1 = (ab - cd\rho)$, $A_2 = (ab\alpha - cd)$, $A_3 = (bc - ad\mu)$, $A_4 = (bc\beta - ad)$, we have

$$\begin{aligned} N(\delta) &= ((ab - cd\rho) + (ab\alpha - cd)\delta)((bc - ad\mu) - (bc\beta - ad)\delta) \\ &= (A_1 + A_2\delta)(A_3 - A_4\delta) \\ &= A_1A_3 - (A_1A_4 - A_2A_3)\delta - A_2A_4\delta^2. \end{aligned} \quad (64)$$

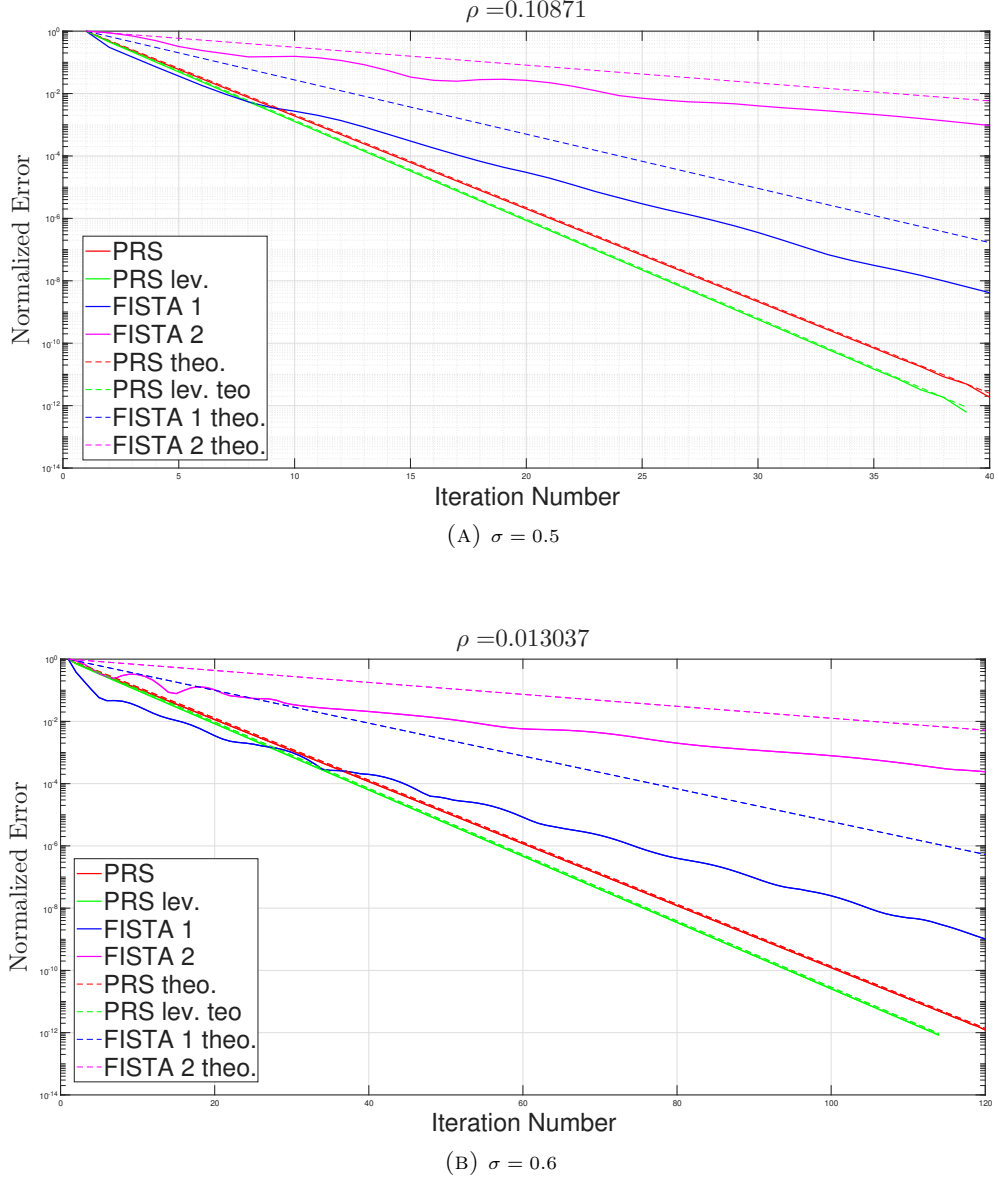


FIGURE 2. Normalized error vs Iteration number.

Moreover, it follows from (63) that

$$\begin{aligned}
 A_1 A_3 &= (ab - cd\rho)(bc - ad\mu) \\
 &= ab^2c - a^2bd\mu - c^2bd\rho + acd^2\rho\mu \\
 &= ac(b^2 + d^2\rho\mu) - bd(a^2\mu + c^2\rho) \\
 &= ac(\rho + \mu + (\alpha + \beta)\rho\mu) - bd((1 + \beta\rho)\mu + (1 + \alpha\mu)\rho) \\
 &= (ac - bd)((1 + \beta\rho)\mu + (1 + \alpha\mu)\rho)
 \end{aligned} \tag{65}$$

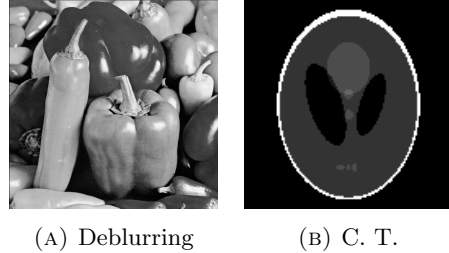
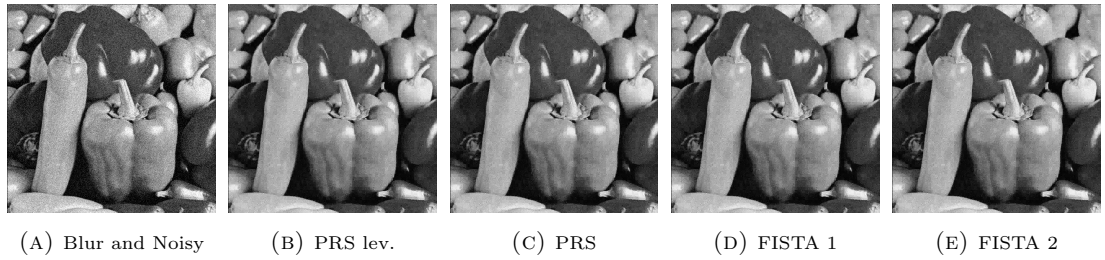
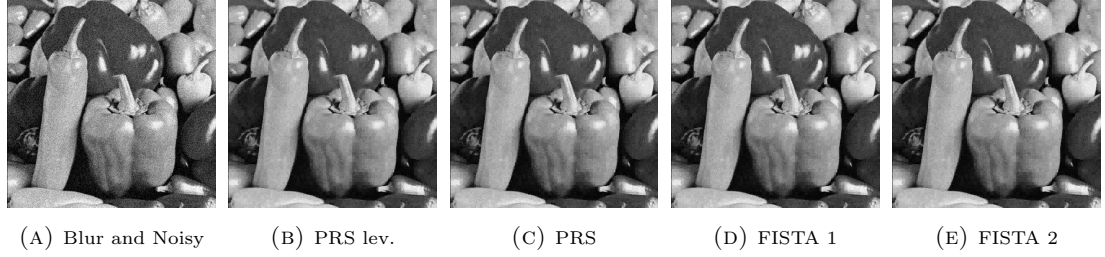


FIGURE 3. Original Images

FIGURE 4. $\sigma = 0.5, \rho = 0.11$ FIGURE 5. $\sigma = 0.6, \rho = 0.013$

and

$$\begin{aligned}
 A_2 A_4 &= (ab\alpha - cd)(bc\beta - ad) \\
 &= ab^2 c \alpha \beta - a^2 b d \alpha - b c^2 d \beta + a c d^2 \\
 &= ac(b^2 \alpha \beta + d^2) - bd(a^2 \alpha + c^2 \beta) \\
 &= ac((\rho + \mu)\alpha\beta + \alpha + \beta) - bd((1 + \beta\rho)\alpha + (1 + \alpha\mu)\beta) \\
 &= (ac - bd)((1 + \beta\rho)\alpha + (1 + \alpha\mu)\beta).
 \end{aligned} \tag{66}$$

Hence, by defining $B_1 = ((1 + \beta\rho)\mu + (1 + \alpha\mu)\rho)$ and $B_2 = ((1 + \beta\rho)\alpha + (1 + \alpha\mu)\beta)$ it follows from (64), (65), and (66) that

$$N(\delta) = (ac - bd) \left(B_1 - \frac{(B_1 A_4 - B_2 A_3)}{A_3 A_4} \delta - B_2 \delta^2 \right), \tag{67}$$

where $A_3 A_4 \neq 0$ because $\beta\mu < 1$. Analogously, we derive

$$D(\delta) = (ac + bd) \left(B_1 - \frac{(B_1 A_4 - B_2 A_3)}{A_3 A_4} \delta - B_2 \delta^2 \right). \tag{68}$$

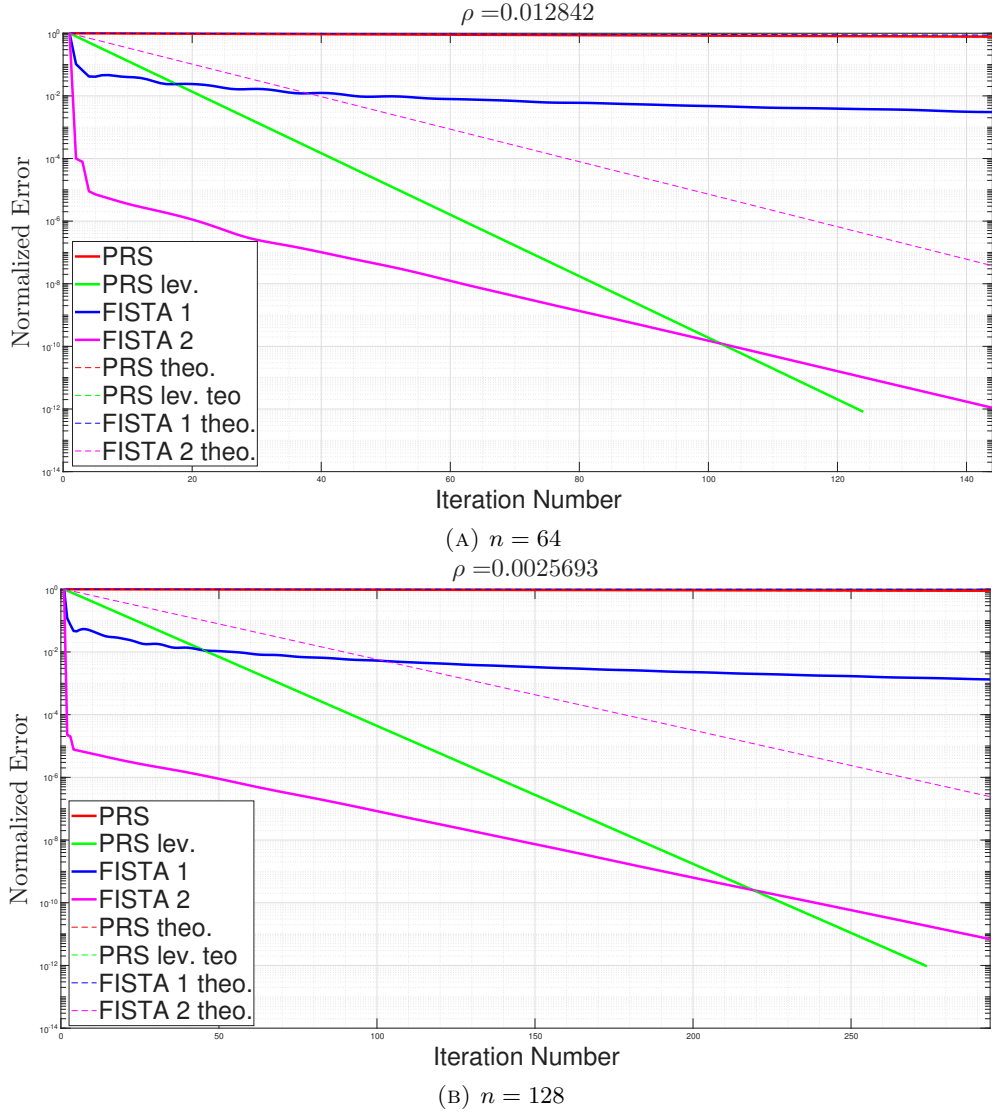
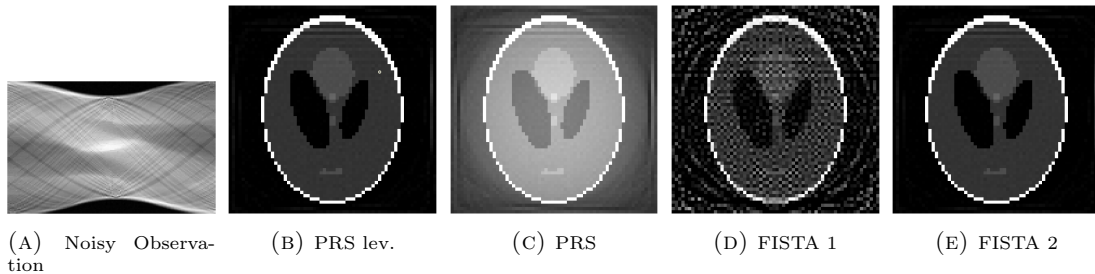
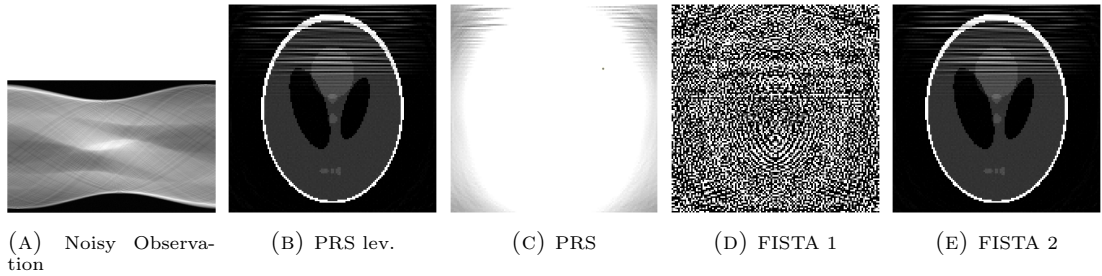


FIGURE 6. Normalized error vs Iteration number.

FIGURE 7. $m = 64$.

FIGURE 8. $m = 128$.

Finally, from (67) and (68) we conclude

$$r(\delta) = \frac{N(\delta)}{D(\delta)} = \frac{ac - bd}{ac + bd} = \frac{\sqrt{(1 + \beta\rho)(1 + \alpha\mu)} - \sqrt{(\alpha + \beta)(\rho + \mu)}}{\sqrt{(1 + \beta\rho)(1 + \alpha\mu)} + \sqrt{(\alpha + \beta)(\rho + \mu)}}$$

and the result follows. \square

6. ACKNOWLEDGMENT

The work of Luis M. Briceño-Arias is supported by Centro de Modelamiento Matemático (CMM), FB210005, BASAL fund for centers of excellence, and FONDECYT 1230257 from ANID-Chile. The work of Fernando Roldán is supported by ANID-Chile under grant FONDECYT Iniciación 11250164.

REFERENCES

- [1] Baillon, J.B., Haddad, G.: Quelques propriétés des opérateurs angle-bornés et n -cycliquement monotones. *Israel Journal of Mathematics* **26**, 137–150 (1977). DOI 10.1007/BF03007664
- [2] Bauschke, H.H., Combettes, P.L.: Convex analysis and monotone operator theory in Hilbert spaces, second edn. CMS Books in Mathematics/Ouvrages de Mathématiques de la SMC. Springer, Cham (2017). DOI 10.1007/978-3-319-48311-5
- [3] Beck, A., Teboulle, M.: A fast iterative shrinkage-thresholding algorithm for linear inverse problems. *SIAM J. Imaging Sci.* **2**(1), 183–202 (2009). DOI 10.1137/080716542. URL <https://doi.org/10.1137/080716542>
- [4] Benamou, J.D., Carlier, G.: Augmented lagrangian methods for transport optimization, mean field games and degenerate elliptic equations. *Journal of Optimization Theory and Applications* **167**(1), 1–26 (2015). DOI 10.1007/s10957-015-0725-9. URL <https://doi.org/10.1007/s10957-015-0725-9>
- [5] Briceño-Arias, L.M., Silva, F.J., Yang, X.: Forward-backward algorithm for functions with locally lipschitz gradient: Applications to mean field games. *Set-Valued and Variational Analysis* **32**(2), 16 (2024). DOI 10.1007/s11228-024-00719-1. URL <https://doi.org/10.1007/s11228-024-00719-1>
- [6] Briceño-Arias, L.M.: Lyapunov analysis for FISTA under strong convexity (2025). URL <https://arxiv.org/abs/2506.11785>
- [7] Briceño-Arias, L.M., Pustelnik, N.: Convergence rate comparison of proximal algorithms for non-smooth convex optimization with an application to texture segmentation. *IEEE Signal Processing Letters* **29**, 1337–1341 (2022). DOI 10.1109/LSP.2022.3179169
- [8] Briceño-Arias, L.M., Pustelnik, N.: Theoretical and numerical comparison of first order algorithms for cocoercive equations and smooth convex optimization. *Signal Processing* **206**, 108,900 (2023). DOI <https://doi.org/10.1016/j.sigpro.2022.108900>. URL <https://www.sciencedirect.com/science/article/pii/S016516842200439X>
- [9] Briceño-Arias, L.M., Kalise, D., Silva, F.J.: Proximal methods for stationary mean field games with local couplings. *SIAM Journal on Control and Optimization* **56**(2), 801–836 (2018). DOI 10.1137/16M1095615. URL <https://doi.org/10.1137/16M1095615>
- [10] Briceño-Arias, L.M., Kalise, D., Kobeissi, Z., Laurière, M., Mateos González, Á., Silva, F. J.: On the implementation of a primal-dual algorithm for second order time-dependent mean field games with local couplings. *ESAIM: ProcS* **65**, 330–348 (2019). DOI 10.1051/proc/201965330. URL <https://doi.org/10.1051/proc/201965330>

- [11] Carlier, G., Chenchene, E., Eichinger, K.: Wasserstein medians: Robustness, pde characterization, and numerics. *SIAM Journal on Mathematical Analysis* **56**(5), 6483–6520 (2024). DOI 10.1137/23M1624786. URL <https://doi.org/10.1137/23M1624786>
- [12] Davis, D., Yin, W.: Faster convergence rates of relaxed peaceman-rachford and admm under regularity assumptions. *Mathematics of Operations Research* **42**(3), 783–805 (2017). DOI 10.1287/moor.2016.0827. URL <https://doi.org/10.1287/moor.2016.0827>
- [13] Douglas, J., Rachford, H.H.: On the numerical solution of heat conduction problems in two and three space variables. *Transactions of the American Mathematical Society* **82**(2), 421–439 (1956). URL <http://www.jstor.org/stable/1993056>
- [14] Eckstein, J., Bertsekas, D.P.: On the Douglas–Rachford splitting method and the proximal point algorithm for maximal monotone operators. *Mathematical Programming* **55**(1), 293–318 (1992). DOI 10.1007/BF01581204. URL <https://doi.org/10.1007/BF01581204>
- [15] Giselsson, P.: Tight global linear convergence rate bounds for Douglas–Rachford splitting. *Journal of Fixed Point Theory and Applications* **19**(4), 2241–2270 (2017). DOI 10.1007/s11784-017-0417-1. URL <https://doi.org/10.1007/s11784-017-0417-1>
- [16] Giselsson, P., Boyd, S.: Linear convergence and metric selection for Douglas–Rachford splitting and ADMM. *IEEE Transactions on Automatic Control* **62**(2), 532–544 (2017). DOI 10.1109/TAC.2016.2564160
- [17] Kak, A.C., Slaney, M.: Principles of Computerized Tomographic Imaging. Society of Industrial and Applied Mathematics (2001)
- [18] Krasnosel'skiĭ, M.A.: Two remarks on the method of successive approximations. *Uspekhi Matematicheskikh Nauk* **10**(1), 123–127 (1955). URL <http://mi.mathnet.ru/eng/rm7954>
- [19] Lions, P.L., Mercier, B.: Splitting algorithms for the sum of two nonlinear operators. *SIAM J. Numer. Anal.* **16**(6), 964–979 (1979). DOI 10.1137/0716071. URL <https://doi.org/10.1137/0716071>
- [20] Mann, W.R.: Mean value methods in iteration. *Proceedings of the American Mathematical Society* **4**(3), 506–510 (1953). URL <http://www.jstor.org/stable/2032162>
- [21] Monteiro, R.D.C., Sim, C.K.: Complexity of the relaxed Peaceman–Rachford splitting method for the sum of two maximal strongly monotone operators. *Comput. Optim. Appl.* **70**(3), 763–790 (2018). DOI 10.1007/s10589-018-9996-z. URL <https://doi.org/10.1007/s10589-018-9996-z>
- [22] Papadakis, N., G., P., Oudet, E.: Optimal transport with proximal splitting. *SIAM Journal of Imaging Sciences* (2013). DOI 10.1137/130920058
- [23] Pascal, B., Pustelnik, N., Abry, P.: Strongly convex optimization for joint fractal feature estimation and texture segmentation. *Applied and Computational Harmonic Analysis* **54**, 303–322 (2021)
- [24] Peaceman, D.W., Rachford Jr., H.H.: The numerical solution of parabolic and elliptic differential equations. *Journal of the Society for Industrial and Applied Mathematics* **3**(1), 28–41 (1955). DOI 10.1137/0103003. URL <https://doi.org/10.1137/0103003>
- [25] Svaiter, B.F.: On weak convergence of the Douglas–Rachford method. *SIAM Journal on Control and Optimization* **49**(1), 280–287 (2011). DOI 10.1137/100788100. URL <https://doi.org/10.1137/100788100>
- [26] van Aarle, W., Palenstijn, W.J., Cant, J., Janssens, E., Bleichrodt, F., Dabovolski, A., Beenhouwer, J.D., Batenburg, K.J., Sijbers, J.: Fast and flexible x-ray tomography using the astra toolbox. *Opt. Express* **24**(22), 25,129–25,147 (2016). DOI 10.1364/OE.24.025129
- [27] van Aarle, W., Palenstijn, W.J., De Beenhouwer, J., Altantzis, T., Bals, S., Batenburg, K.J., Sijbers, J.: The astra toolbox: A platform for advanced algorithm development in electron tomography. *Ultramicroscopy* **157**, 35–47 (2015). DOI <https://doi.org/10.1016/j.ultramic.2015.05.002>
- [28] Zeng, G., Gullberg, G.: A ray-driven backprojector for backprojection filtering and filtered backprojection algorithms. In: 1993 IEEE Conference Record Nuclear Science Symposium and Medical Imaging Conference, pp. 1199–1201 (1993). DOI 10.1109/NSSMIC.1993.701833